

Observations of comet Shoemaker–Levy 9 from Japal–Rangapur Observatory

R. Vasundhara¹, Pavan Chakraborty¹, R. Rajamohan¹, J. C. Bhattacharyya¹, G. Som Sunder², P. Vivekananda Rao², R. Swaminathan² and B. Lokanadham²

¹Indian Institute of Astrophysics, Bangalore 560 034, India

²Department of Astronomy, Osmania University, Hyderabad 500 007, India

Preliminary results of observations of comet Shoemaker–Levy 9 from Rangapur Observatory during 21–22 January 1994 are presented. Astrometric positions of resolved fragments were estimated using multiple triangulations of stars in HST Guide star catalogue. Tails from individual fragments could be resolved up to about 10 arcsec. An ambient dusty region extending to about 17–20 arcsec on the anti-sun direction of the cometary train is evident on all the frames.

THE discovery of the periodic comet Shoemaker–Levy 9 (SL9) as a squashed comet by Eugene and Carolyn Shoemaker and David Levy in late March 1993 has spurred considerable interest in the planetary wing of the astronomical community¹. Subsequent observations

showed the object to be, in fact, a train of individual nuclei¹. Images taken from Mauna Kea Observatory by Jewitt *et al.* showed about 20 separate pieces strung out like a string of pearls^{2,3}. Orbit computations by Marsden⁴ indicated that the individual pieces of the cometary train are the fragments of a progenitor comet which made a close approach to Jupiter at a height of about 1/4 of the planetary radius from the cloud top, and was tidally disrupted. These chunks of cometary pieces are in elongated orbit around Jupiter and are predicted to collide with the planet between 16 and 22 July 1994. Observations were carried out to obtain the astrometric positions and to study the morphology of the tail at the Japal–Rangapur Observatory. This paper discusses the preliminary results of the analysis.

The observations were carried out at the prime focus of 122 cm *f*/3.5 reflector at Japal–Rangapur Observatory (5 h 14 min E, 17 deg 6 min N). A Baker corrector with a Ross lens assembly provided a corrected field of about 13' × 13' on the CCD detector of 512 × 512 pixels. The observations were made in integrated light. A large number of field stars were registered in the moderately large field on the CCD frame. Stars in the HST Guide star catalogue⁵ were identified and used as reference stars for multiple triangulations. The positions of the objects were measured using the imexamine package of IRAF*

Table 1. Positions of fragments of comet Shoemaker–Levy 9

Date Jan. 94	Fragment	$\alpha(2000.0)$	$\delta(2000.0)$	$\alpha(2000.0)$	$\delta(2000.0)$
		Observed		Predicted	
21.9295138	G (15)	14 32 35.750	– 15 48 42.59	14 32 35.772	– 15 48 44.41
	Q (7)	14 32 31.466	– 15 49 13.69	14 32 31.525	– 15 49 14.99
	S (5)	14 32 30.043	– 15 49 24.36	14 32 30.025	– 15 49 24.48
	W (1)	14 32 28.856	– 15 49 33.15	14 32 28.895	– 15 49 32.88
21.9394675	E (17)	14 32 37.424	– 15 48 34.20	14 32 37.101	– 15 48 37.97
	G (15)	14 32 35.990	– 15 48 43.59	14 32 36.032	– 15 48 45.58
	K (12)	14 32 34.088	– 15 48 57.43	14 32 34.232	– 15 48 59.37
	L (11)	14 32 33.242	– 15 49 03.24	14 32 33.323	– 15 49 05.67
	Q (7)	14 32 31.722	– 15 49 14.35	14 32 31.783	– 15 49 16.16
	S (5)	14 32 30.234	– 15 49 24.18	14 32 30.284	– 15 49 25.66
	E (17)	14 32 37.695	– 15 48 34.91	14 32 37.513	– 15 48 37.54
21.955243	G (15)	14 32 36.410	– 15 48 45.56	14 32 36.443	– 15 48 47.44
	H (14)	14 32 35.642	– 15 48 49.11	14 32 35.604	– 15 48 53.64
	K (12)	14 32 34.524	– 15 48 59.02	14 32 34.644	– 15 49 01.23
	L (11)	14 32 33.479	– 15 49 05.35	14 32 33.734	– 15 49 07.53
	Q (7)	14 32 32.175	– 15 49 15.82	14 32 32.194	– 15 49 18.03
	S (5)	14 32 30.695	– 15 49 27.08	14 32 30.695	– 15 49 27.52
	W (1)	14 32 29.630	– 15 49 33.87	14 32 29.565	– 15 49 35.92
	E (17)	14 33 02.974	– 15 50 27.53	14 33 02.726	– 15 50 30.89
	G (15)	14 33 01.616	– 15 50 39.00	14 33 01.651	– 15 50 40.87
	K (12)	14 32 59.754	– 15 50 52.39	14 32 59.842	– 15 50 54.82
22 9320601	L (11)	14 32 58.853	– 15 50 59.29	14 32 58.927	– 15 51 01.17
	Q (7)	14 32 57.408	– 15 51 09.62	14 32 57.379	– 15 51 11.76
	S (5)	14 32 55.810	– 15 51 21.10	14 32 55.864	– 15 51 21.36
	K (12)	14 33 00.209	– 15 50 55.90	14 33 00.370	– 15 50 57.20
	L (11)	14 32 59.400	– 15 51 00.53	14 32 59.456	– 15 51 03.55
	Q (7)	14 32 57.866	– 15 51 12.72	14 32 57.907	– 15 51 14.14
	S (5)	14 32 56.569	– 15 51 22.74	14 32 56.392	– 15 51 23.74

*IRAF is distributed by the National Optical Astronomy Observatories which is operated by the Association of Universities Inc. (AURA) under co-operative agreement with the National Science Foundation

Table 2. (O-C) in right ascension and declination of the fragments

Fragment	(O-C) α (arcsec)	(O-C) δ (arcsec)
E	0.54 ± 3.3	-3.25 ± 0.41
G	-0.50 ± 0.08	-1.89 ± 0.04
K	-1.92 ± 0.27	-1.97 ± 0.28
L	-1.75 ± 0.81	-2.38 ± 0.28
Q	-0.45 ± 0.27	-1.78 ± 0.20
S	-0.90 ± 0.51	-0.66 ± 0.28
W	-0.78 ± 0.27	-1.16 ± 0.27

SL9 1994/01/21 22:55:33 UT

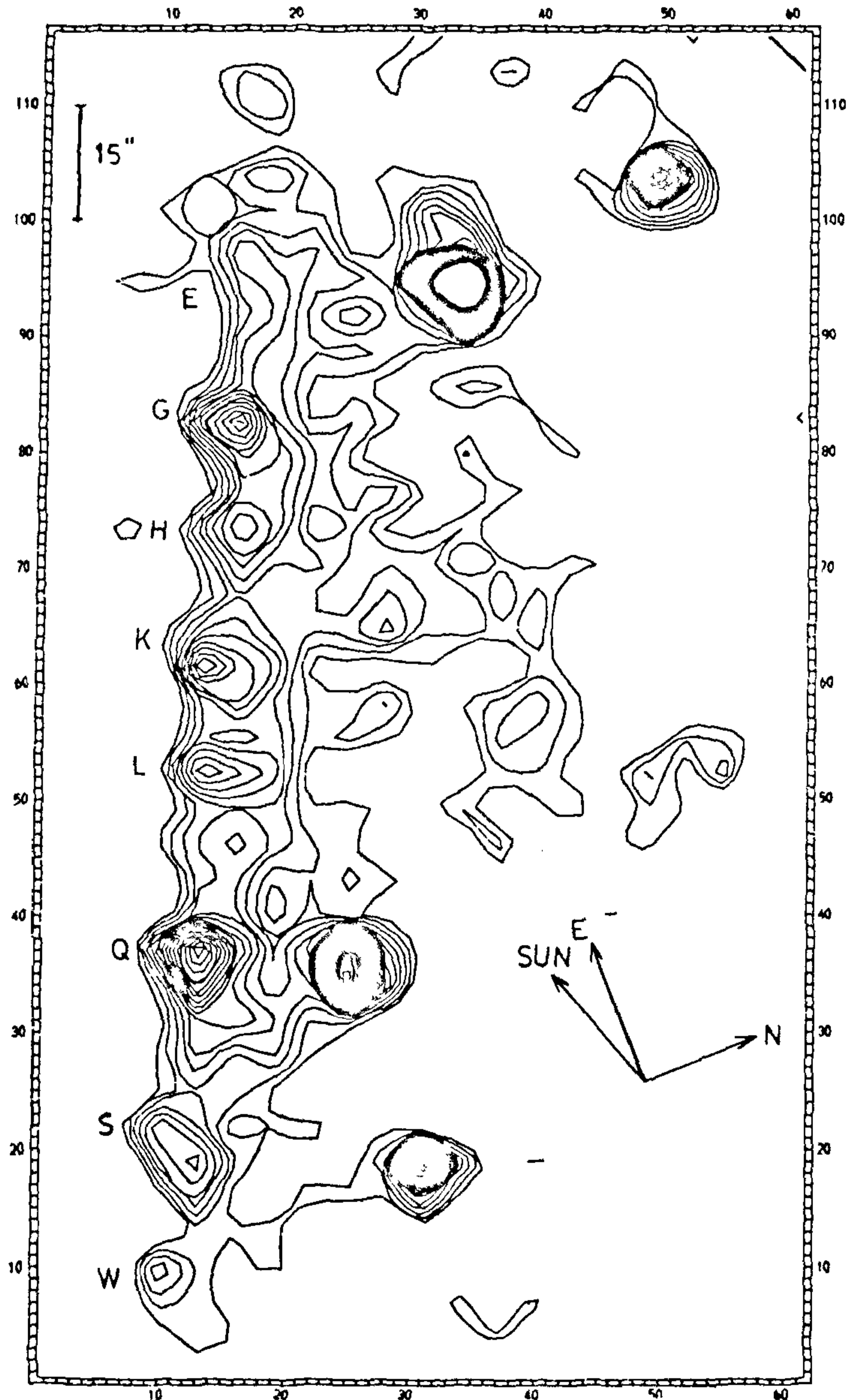


Figure 1a.

SL9 1994/01/22 22:22:10 UT [R]

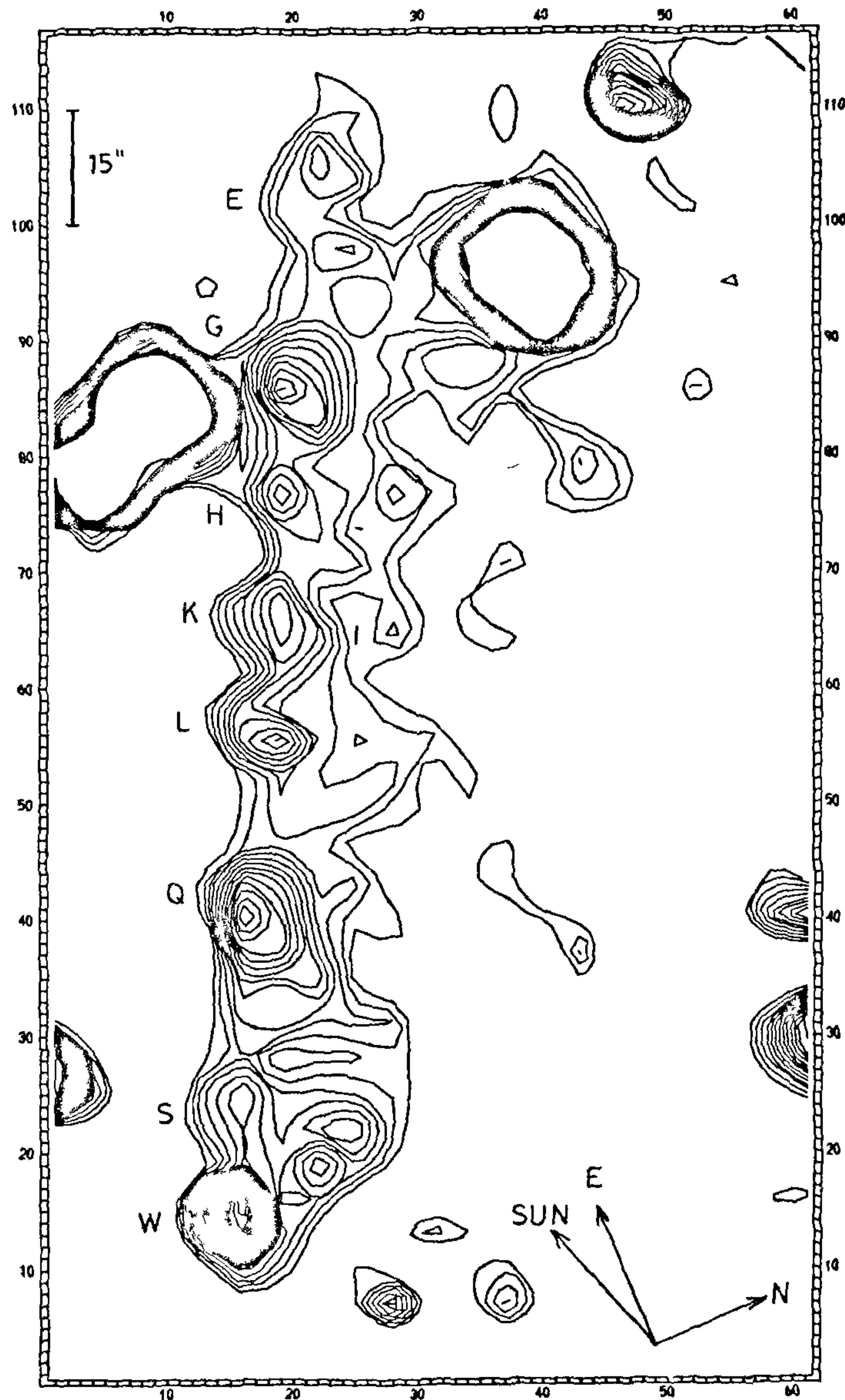


Figure 1. Contour plots of dust around the fragments in images obtained on *a*, 21.955243 and *b*, 22.9320601. Thirty isophots (at equal intensity intervals) are plotted in each case between $19.80 \text{ mag/arcsec}^2$ and $19.75 \text{ mag/arcsec}^2$ to bring out the faint structures in the tails

at the SUN Workstation at the Indian Institute of Astrophysics, Bangalore. The individual nuclei of the comet were identified according to the standard nomenclature. The 2000.0 coordinates of the fragments are given in Table 1. These are compared with the predicted positions by Yeomans and Chodas⁶, who used the positions of the fragments till 12 December 1993.

The (O-C) in right ascension and declination for the fragments E, G, K, L, Q, S and W are given in Table 2. Except for the fragment E, the positions on 21-22 January 1994 are found to be to the west and south of the extrapolated predicted positions.

Isointensity contours of the region near the comet are plotted in Figure 1 *a,b*. The direction of the sun projected

on the sky plane is shown in each case. Tails from individual fragments could be resolved up to about 10 arcsec. An ambient dusty region extending to about 30 arcsec on the anti-sun direction of the cometary train is evident on all the frames. At the comet's distance this equals a projected linear distance of about 120,000 km.

A comparison of the image of SL9 with that on 29 May 1993, shows that the morphology of the dusty region surrounding SL9 drastically changed⁷. For example, the dust envelope has significantly thinned and the wings extending on either side of the train are missing. The dynamics of the dust in the tail of the comet SL9 is complicated. For normal comets which develop tails while approaching the Sun, the syndynes and synchrones⁸ can be determined entirely from the grain sizes, their density and optical properties. This is so because the ratio of the radiation pressure force to the gravitational force depends only on the comet's heliocentric distance. In case of SL9, while the radiation pressure on a grain of given size and density is very nearly the same, the gravitational force which is governed by three-body dynamics is not. Analysis of the tail

structure to derive information on the nature of the grains and their size distribution or to look for evidences of bursts or jets requires detailed modelling⁹. The limited data obtained on two successive days precludes such an attempt.

1. I.A.U.C. No. 5725, 1993.
2. I.A.U.C. No. 5730, 1993.
3. Jewitt, J., Luu, J. and Chen, J., *Bull. Am. Astron. Soc.*, 1993, **25**, 1042.
4. I.A.U.C. No. 5906, 1993.
5. Lasker, B. M., Sturch, C. R., McLean, B. J., Russell, J. L., Jenkner, H. and Shara, M. M., *Astron. J.*, 1990, **99**, 2019-2058.
6. Yeomans, D. K. and Chodas, P. W., 1993, private communication (orbit ref. 12/17/93)
7. Kameswara Rao, N., Mayya, Y. D., Eswar Reddy, B. and Prabhu, T. P., *Bull. Astron. Soc. India*, 1993, **21**, 221-222.
8. Finston, M. F. and Probst, R. F., *Astrophys. J.*, **154**, 327-352.
9. Finston, M. F. and Probst, R. F., *Astrophys. J.*, **154**, 353-380.

ACKNOWLEDGEMENTS. This work was supported in part by funding from the Department of Science and Technology, Government of India, and the Smithsonian Institutes, Washington.

Received 1 July 1994, revised accepted 1 October 1994

Burst vortex flow-field on a delta wing—A numerical simulation using Euler equations

Anand Kumar

Computational and Theoretical Fluid Dynamics Division, National Aerospace Laboratories, Bangalore 560 017, India

A numerical simulation of vortex breakdown on a delta wing is carried out. Flow-field within and around vortex breakdown is presented to illustrate the vortex breakdown phenomenon.

WHEN a delta wing is placed in a flow at an incidence, flow separates along the leading-edge and vorticity is shed, which rolls up to form coiled vortex sheets above the wing, with a core of high vorticity. The suction in the vortex core induces additional lift which is exploited aerodynamically, as in the design of modern fighter aircraft. An increase in the incidence leads to a stronger vortex. If the vortex is sufficiently strong, a sudden change in the structure of the vortex core, known as vortex breakdown or vortex bursting, occurs somewhere along the vortex axis. Vortex breakdown is characterized by a sudden drop in suction and a pronounced alteration

of velocity field in the vortex core. The two types of vortex breakdown that occur on delta wings are called bubble type and spiral type. Due to its importance in aeronautical and non-aeronautical applications, vortex breakdown, first observed by Peckham and Atkinson¹, is an active area of experimental and theoretical research. A recent review of vortex breakdown is presented by Delery².

Even after three decades of research, the underlying mechanisms leading to vortex breakdown are still not well understood, although several theories of vortex breakdown have been proposed³. Here, based on Euler equations, numerical simulation of burst vortex flow-field over a sharp leading-edge delta wing is carried out, with the hope that some of the observations made here will help understand the vortex breakdown mechanisms better. The vortex breakdown phenomenon is highlighted by presenting the computed flow-field. The use of Euler equations for our study of vortex breakdown is based on the experimental observations⁴ that the vortex breakdown is almost independent of viscous effects. We consider a sharp leading-edge wing since the primary separation is then fixed along the leading-edges. The vortex sheet shed from the sharp leading-edge which rolls up to form the primary vortex is well modelled